CHEMISTRY
A EUROPEAN JOURNAL

DOI: 10.1002/chem.201001439

Prediction of EPR Spectra of Liquid Crystals with Doped Spin Probes from Fully Atomistic Molecular Dynamics Simulations: Exploring Molecular Order and Dynamics at the Phase Transition

Egidisus Kuprusevicius,[a] Ruth Edge,[b] Hemant Gopee,[a] Andrew N. Cammidge,[a] Eric J. L. McInnes,[b] Mark R. Wilson,[c] and Vasily S. Oganesyan*[a]

Molecular dynamics (MD) simulations are becoming an important tool for modelling complex molecular systems at the atomistic scale and for understanding the various chemical, physical and spectroscopic properties of soft matter[1] and liquid crystals in particular.[2–4] Increasingly, atomistic simulations have predictive power and can guide the design of novel functional materials. In this respect it is important to test MD predictions against available experimental methods, such as advanced spectroscopic techniques. Recently, the use of nitroxide spin labels as paramagnetic probes for electron paramagnetic resonance (EPR) spectroscopy has attained wide applicability.[5] EPR with spin probes (SP) is widely used to test structural properties and molecular mobility of numerous complex molecular systems, such as proteins and protein–protein complexes, DNA/RNA, polymers, lipids, solid films, nanostructures and also liquid crystals (LC).[6]

Nitroxide spin probes can be readily introduced into LCs to probe the order and dynamics of mesogens in different phases.[4,7] Scheme 1 shows an example of a cholesteric nitroxide SP typically used for calamitic (rod-shaped) LCs. The nitroxide radical is chemically relatively stable and has an EPR spectrum consisting of an almost isotropic **g** tensor ($g_{xx}=2.0088$, $g_{yy}=2.0061$, $g_{zz}=2.0027$)[4] with anisotropic hyperfine coupling (**A** tensor: $A_{xx}=5.9$ G, $A_{yy}=5.9$ G, $A_{zz}=31.7$ G)[4] to a single ^{14}N nuclear spin $I=1$ that gives a three derivative shape line spectrum at the X-band. The three lines $\omega(t)^m=(g_{zz}(\Omega(t))\beta B+A_{zz}(\Omega(t)m)/\hbar$ are the functions of the calculated MD trajectory $\Omega(t)$ where A_{zz} and g_{zz} are effective g and hyperfine coupling constants calculated by using the principle values for **g** and **A** according to the previously described procedure.[4,8,9]

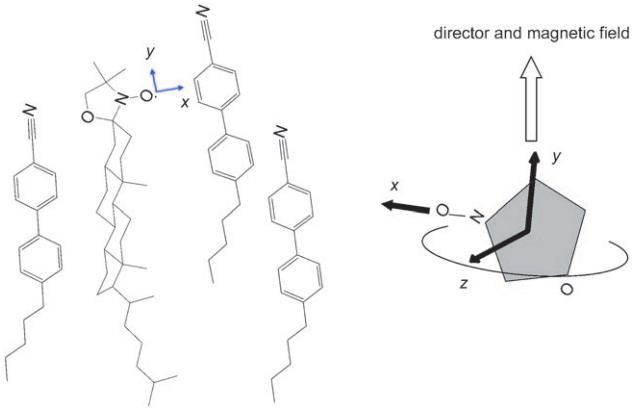

Scheme 1. A schematic representation of the cholesteric spin probe surrounded by 4-cyano-4-*n*-pentylbiphenyl (5CB) LC molecules (*x*, *y* and *z* vectors show the orientation of magnetic axes relative to both the nitroxide head group and to the direction of director and magnetic field in nematic phase).

The variables β, $\hbar$ and B are the Bohr magneton, the Planck constant and the magnetic field, respectively and $m=\pm1$, 0. An important feature of EPR spectroscopy is that it can resolve the details of molecular re-orientational dynamics over time scales of 10^{-11}–10^{-7} s.[5] The lines are sensitive to local dynamics and the order of the probe, and their shapes can range from the completely averaged narrow lines in the case of fast isotropic motion to broad asymmetric features in the case of the "frozen" limit. A vari-

[a] E. Kuprusevicius, Dr. H. Gopee, Dr. A. N. Cammidge, Dr. V. S. Oganesyan
School of Chemistry, University of East Anglia
Norwich, NR4 7TJ (UK)
Fax: (+44) 1603-592003
E-mail: v.oganesyan@uea.ac.uk

[b] Dr. R. Edge, Prof. E. J. L. McInnes
School of Chemistry, University of Manchester
Manchester, M13 9PL (UK)

[c] Prof. M. R. Wilson
Department of Chemistry, Durham University
University Science Laboratories, South Road
Durham, DH1 3 LE (UK)

ety of different shapes can be observed in between these two limiting cases. They are predetermined by three factors: i) rotational diffusion (correlation time) of the nitroxide head group, ii) motional restrictions imposed by the surrounding mesogens (ordering potential) and iii) global order imposed by the liquid-crystal state. Information about all three contributions can be depicted from the analysis of EPR spectra, which are very sensitive to the changes in dynamics and the order of the SP within the LC system.

Previously, we have reported an effective method for calculation of EPR spectra from a single truncated dynamical trajectory of a spin label or probe.[8] It has been shown that an accurate simulation can be achieved from a single MD trajectory provided that the autocorrelation function of reorientational motion of the spin label has completely relaxed. This approach has opened the prospect of the simulation of EPR spectra entirely from MD trajectories of real molecular structures with introduced spin probes. Such a technique does not require additional modelling of the spin probe's dynamics or fitting of spectra by using adjustable parameters, and therefore, greatly simplifies the interpretation and analysis of EPR spectra. It also allows for unambiguous conclusions to be reached for the order and the dynamics in soft matter systems. Most recently, we have reported the first successful coarse-grained (CG) MD simulation of a LC with doped cholesteric SP.[4]

In this communication, we present the first prediction of EPR spectra for a liquid crystal with a doped spin probe from MD simulations at the fully atomistic level. The EPR predictions focus particularly on the LC states along the nematic–isotropic (N–I) phase-transition curve and are tested against the measured EPR spectra. MD simulations were performed on a system of 4-cyano-4-*n*-pentylbiphenyl (5CB) molecules consisting of 141 randomly arranged (head to tail) molecules in a cubic box of 4.5 nm dimensions with cubic periodic boundary conditions. For each temperature, the system, initially composed of 5CB molecules, was equilibrated for 50 ns followed by the doping of the SP at the central position of the box. The system was further equilibrated for another 30 ns followed by long production runs for EPR simulations. Figure 1 shows the time evolution of the LC order parameter over the course of typical MD runs.

It is important to mention that during the long equilibration runs it was possible to achieve a growth of a pure nematic state from a completely isotropic one (as shown by the red line in Figure 1a)) and vice versa, demonstrating thermodynamic stability of the LC states. Such behaviour in model systems has been observed previously for nematic LC and LC mixtures, albeit quite rarely.[3,10] In our simulations, an exception was a very narrow region ($\Delta T \approx 2$–3 K) around the N–I phase change, where the dynamics of the LC order parameter indicate the existence of metastable states of the mesogens. In particular, for $T = 385$ K a collapse of the initially partially ordered state to a completely isotropic one has been observed followed by the re-growth back to a partial nematic (red line in Figure 1b)). The detection of such events was possible by running relatively long trajectories of

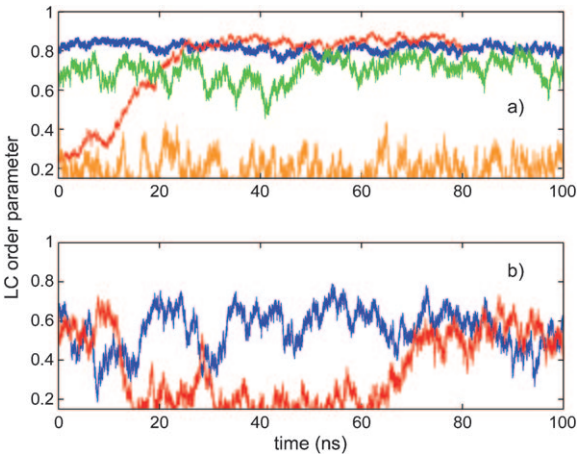

Figure 1. Time evolution of the LC order parameter at different simulation temperatures. a) The blue, green and orange lines correspond to $T =$ 320, 360 and 400 K, respectively; the red line represents the growth of a nematic phase from a purely isotropic one at 320 K. b) The blue and red lines correspond to $T = 380$ and 385 K, respectively.

100 ns. The significance of such molecular behaviour in relation to the observed features in the EPR spectrum is discussed below.

Figure 2 shows the phase diagram of 5CB based on the temperature dependences of three order parameters calculated from MD trajectories. Note, that our MD simulations

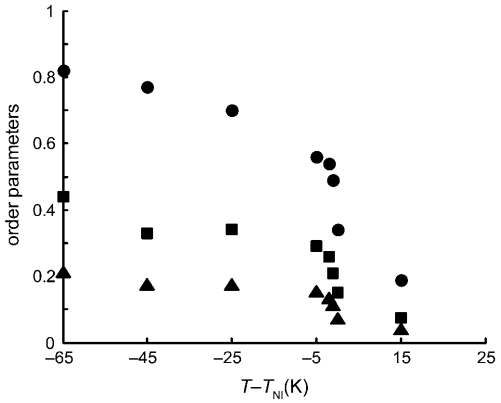

Figure 2. Variation of calculated LC and SP order parameters at different temperatures. Order parameters for LC 5CB (S_{LC}) and the y (S_y) and z (S_z) magnetic axes of the nitroxide probe are shown by circles, cubes and triangles, respectively.

have indicated the systematic shift in phase-transition temperature of ≈ 75 K compared to the experimental one that is 308 K. The N–I clearing point is extremely sensitive to the molecular force field used. For example, very small differences from the experimental density are known to lead to quite large changes in the phase-transition temperature. A systematic shift in temperature is a common observation in MD simulations.[11] In terms of T_{err}/T_{NI}, ($T_{err} = T_{NI}$(calcd)-T_{NI}-(expl)), these changes are small but in comparison with real systems can be as large as 80–100 K.[11] Therefore, an effec-

tive way to compare the simulated and experimental data is to use either a T/T_{NI} or a $T-T_{NI}$ scale.[11]

A second-rank ordering tensor $Q_{ij} = <1/2(3u_iu_j-\delta_{ij})>$, where **u** is a chosen molecular unit vector and δ_{ij} is Kronecker's delta, has been used to measure long-range orientational ordering in the system. Order parameters are calculated by diagonalising the tensor and the director is given by the maximal eigenvalue. Three types of order parameters are calculated in the 5CB–spin probe composite system. One is defined by the core vector of the 5CB molecules yielding the director, whereas the other two are related to the y and z magnetic axes of the nitroxide head group of the spin probe. For the LC the ordering tensor is averaged over the ensemble and the time, whereas for the two magnetic axes of the SP the order parameters are obtained from time averages. There is a strong correlation among all three order parameters: S_{LC} being the largest as it is related to the core vector of the solvent molecules, whereas S_y is associated with the flexible nitroxide group. Finally, the z axis being perpendicular to the ring (see Scheme 1) is associated with the axial dynamics of the probe, which results in the lower value of the corresponding order parameter S_z.

At the X-band the sensitivity of the EPR line shape is pre-determined by the anisotropy of the hyperfine coupling of ^{14}N. This would lead to a strong dependence of the observed shape of the EPR spectrum on the direction of the magnetic field relative to the principle axes of the hyperfine coupling tensor (see Scheme 1). In our system, the magnetic field is set along the orientation of the director. Figure 3a shows the predicted EPR spectrum for a pure nematic phase. It is characterised by three closely-positioned narrow lines. In the N phase the magnetic field on average is lying in the plane of the nitroxide ring (see Scheme 1). For such orientations of the field the distance between the outer resonance field positions is approaching $2A_{xx/yy}$. In addition, the axial director distribution around the direction of the magnetic field in this state has a bandwidth of $\approx$15°, which is consistent with the observed narrow shapes of the lines.[4] This state is also characterised by the highest value of the order parameters (Figures 1 and 2).

Figure 4 shows the autocorrelation functions for several temperatures calculated from the associated MD trajectories. One can see that all correlation functions of the SP completely relax over times <7 ns indicating that the probe's dynamics is stationary and that the MD–EPR simulation method is readily applicable. This criteria is also satisfied for all temperatures except $T=385$ K, the mid point of the transition curve, which at longer times has slow oscillation around 0 with a period of $\approx$50 ns.

Upon increasing the temperature, the system gradually becomes less ordered as can be seen from the changes of the order parameters shown in Figures 1 and 2. This is also reflected in the shape of the EPR spectrum with the distances between the hyperfine lines increasing and the shapes broadening. Drastic changes of the shape of the EPR spectrum are observed at the phase transition. Shifts to the left and right of the outer positive and negative peaks, respectively, are seen at the simulation temperature $T=380$ K indicating increasing contributions to the resonance field positions from off-plane orientations of the magnetic field. At $T=385$ K the most significant change in the shape of the EPR spectrum is observed (Figure 5).

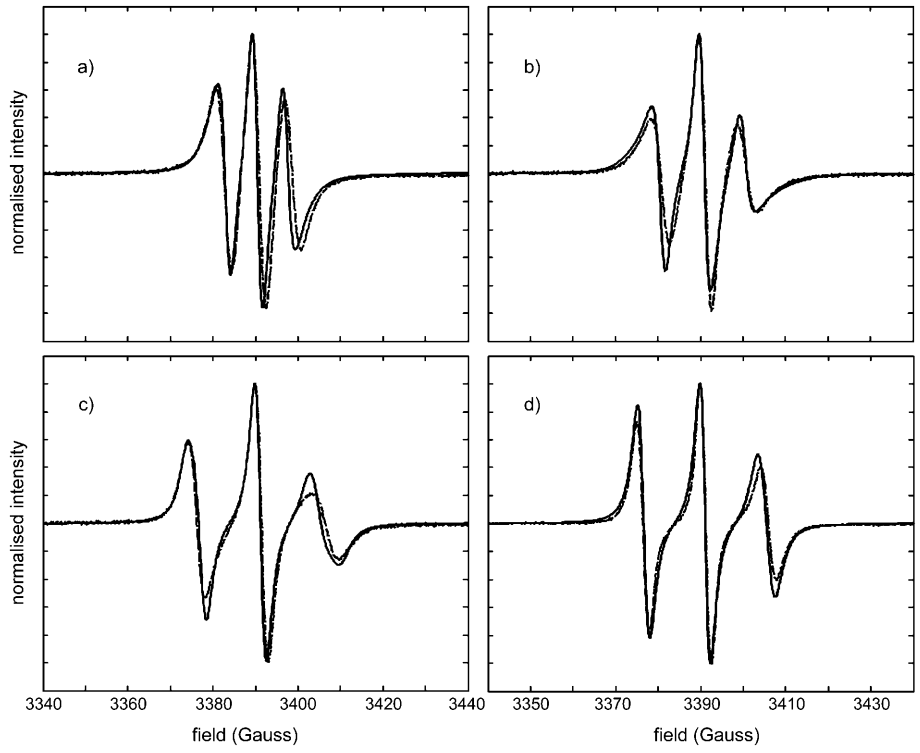

Figure 3. Comparison of simulated (——) and measured (-•-•-) EPR spectra at different values of $T-T_{NI}$. a) $T-T_{NI}=-25$, b) $T-T_{NI}=-2$, c) $T-T_{NI}=2$ and d) $T-T_{NI}=15$ K.

Our EPR measurements have shown that this characteristic shape maintains only for a very narrow temperature interval ($\Delta T=1$ K). An associated MD trajectory is shown in Figure 1b (red line). One can see that at the start of the MD run the system is partially ordered with the order parameter $S_{LC}\approx0.6$. At approximate time, $t=$ 15 ns, the system clears to the isotropic state with an order parameter $S_{LC}\approx0.15$, and at $t=$ 70 ns a nematic phase is regrown. Thus, the system is metastable and is characterised by a slow dynamical exchange between two distinct phases. This is confirmed by the calculated autocorrelation function

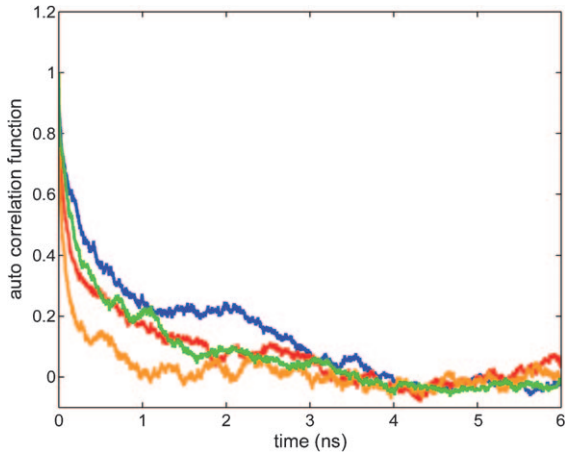

Figure 4. Autocorrelation functions $<\Delta\omega^0(0)\Delta\omega^0(t)>$ of the SP calculated from single MD trajectories generated at different temperatures. Green, blue, red and orange lines correspond to 360, 380, 387 and 400 K, respectively.

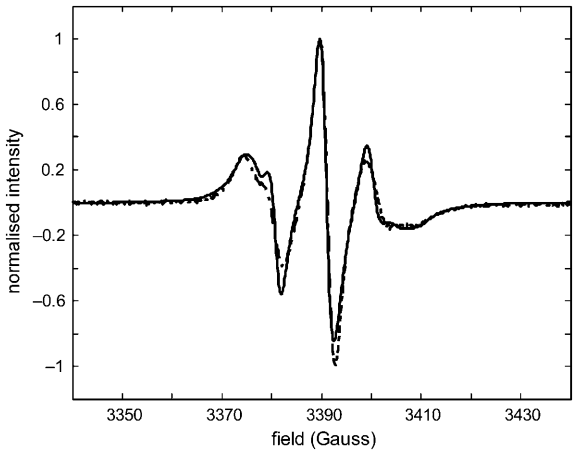

Figure 5. Comparison of simulated (——) and measured (–•–•) EPR spectra at the corresponding temperatures of the critical point on the phase-transition curve, $T-T_{NI}=0$ K.

for the entire length of the MD trajectory, which shows oscillatory behaviour at longer times. These data indicate that the slow dynamical contribution responsible for the interconversion of phases has not completely relaxed and the overall dynamics of the spin probe is non-stationary. However, this exchange process is too slow on the EPR timescale and therefore, sections of the MD trajectory associated either with isotropic or partially ordered states can been used separately in order to provide independent contributions to the overall EPR spectrum.[8] The simulated EPR spectrum is in excellent agreement with the experimental one assuming 30% and 70% contributions from disordered and ordered states, respectively (Figure 5). Figure 3c shows that at a simulation temperature of 387 K ($T-T_{NI}=2$ K) the observed and calculated (from MD) spectra have a specific shape, which is explained as being a result of a partially restricted local motion of the probe. This motion is partly averaged out by superimposing slow diffusional dynamics of the disordered solvent molecules. At this temperature the order parameter of the LC is substantially reduced and the director distribution function is assumed to be isotropic. When the system reaches completely isotropic order at $T\geq$ 395 K (Figure 3d) the fast dynamics of the probe averages out almost completely the hyperfine coupling and the distance between the lines reaches its maximal values. At the same time, all order parameters approach their lowest values.

In conclusion, for the first time we have carried out fully atomistic MD simulations to predict EPR spectra of a nematic LC with doped SP for different LC states across the N–I phase-transition curve. EPR spectra predicted directly from single 100 ns MD trajectories are in agreement with the experiment. A combination of MD and EPR approaches has revealed that at the N–I critical transition point the LC system is metastable and undergoes a dynamical exchange between disordered and partially ordered states. This type of the bulk behaviour is observed in MD simulations on the 100 ns timescale within a narrow temperature interval and is confirmed by EPR experiments. Those two states contribute independently to the overall EPR spectrum and their relative contributions (amounts of time spent in each state) can be estimated. Upon further increase of the temperature by approximately 2 K, the system rapidly collapses into a completely isotropic state. This report shows that a unique combination of atomistic MD simulations and the sensitivity of EPR spectroscopy have an advantage of providing a new level of detail for molecular motions and molecular order in complex systems, such as LC, where nanosecond dynamics of metastable states at the phase transition can be resolved. Our novel MD–EPR approach brings together theory and experiment and offers a rigorous test bed for state-of-the-art MD modelling.

Computational Section

All MD simulations were performed by using the GROMACS 3.3 software package.[12] An all-atom approach was adopted based on the OPLS-AA force field. The force field parameters for 5CB molecule have been reported previously.[10] The relevant parameters for the spin probe have been developed by using a combination of the OPLSS-AA force field and the density functional theory calculations at the B3LYP/6-31G** level by using the Gaussian 03 program.[13] The charge distribution for the head group of the spin probes was obtained by using the CHELPG scheme.[10] All MD simulations were carried out in the *NPT* ensemble ($P=1$ atm, $N=$number of atoms and $T=$temperature) with Berendsen pressure and temperature couplings[14] employed with a relaxation time of 1.0 and 0.1 ps, respectively. A grid neighbour searching with a cut-off radius of 1.0 nm and cubic periodic boundary conditions was employed to generate a pair list of the neighbouring atoms for the non-bonded interactions. Bond lengths were constrained by using the LINCS procedure[15] with the time step of 2 fs. Van der Waals interactions were truncated by using a cut-off of 1.4 nm, whereas long-range electrostatic interactions were handled by a particle-mesh Ewald algorithm with a Coulomb cut-off radius of 1.0 nm.[16,17]

EPR spectra were calculated from single 100 ns MD trajectories according to a procedure described previously.[4,8] In brief, contributions from

each of the three hyperfine lines are calculated as the Fourier transform of the transverse magnetisation generated from an MD trajectory. The de-phasing of the magnetisation is caused by the modulation of $\Delta\omega^m(t)$ due to the re-orientational dynamics of the spin probe, which is characterised by the autocorrelation function $<\Delta\omega^m(0)\Delta\omega^m(t)>$ where $\Delta\omega^m(t)=\Delta\omega^m(t)-\bar{\omega}^m$ and $\bar{\omega}^m$ is a stationary limit reached by the statistically averaged frequency. An in-house written program was used for the simulation and analysis of EPR spectra. In all simulations homogeneous line broadening was accounted by the relaxation parameter $T_2=0.18$ μs as described previously.[4]

Experimental Section

Samples of 5CB LC with doped spin probe were prepared according to the previously described procedure.[4] EPR spectra were measured using an X-band (9.5 GHz) Bruker EMX spectrometer equipped with the digital temperature control system for high temperature measurements using a heated flow of nitrogen gas (Manchester EPR National Service). After being placed inside the EPR cavity the sample was first heated up to 320 K then slowly cooled down to the desired temperature in the presence of magnetic field.

Acknowledgements

The authors wish to thank EPSRC for providing funding under grant EP/H020411/1. V.S.O. also thanks EPSRC for an Advanced Fellowship and UEA for access to high performance computer cluster. M.R.W. wishes to thank Durham University for time on its (hamilton) supercomputer facility.

Keywords: EPR spectroscopy · liquid crystals · molecular dynamics · phase transitions · spin probes

[1] a) C. Peter, K. Kremer, *Soft Matter* **2009**, *5*, 4357; b) M. R. Wilson, *Chem. Soc. Rev.* **2007**, *36*, 1881.
[2] a) D. A. Case, *Acc. Chem. Res.* **2002**, *35*, 325; b) A. J. Ilott, S. Palucha, A. S. Batsanov, M. R. Wilson, P. Hodgkinson, *J. Am. Chem. Soc.* **2010**, *132*, 5179; c) J. Peláez, M. R. Wilson, *Phys. Rev. Lett.* **2006**, *97*, 267801; d) D. Andrienko, V. Marcon, K. Kremer, *J. Chem. Phys.* **2006**, *125*, 124902; e) M. R. Wilson, *Int. Rev. Phys. Chem.* **2005**, *24*, 421.
[3] G. Tiberio, L. Muccioli, R. Berardi, C. Zannoni, *ChemPhysChem* **2009**, *10*, 125.
[4] V. S. Oganesyan, E. Kuprusevicius, H. Gopee, A. N. Cammidge, M. R Wilson, *Phys. Rev. Lett.* **2009**, *102*, 013005.
[5] L. J. Berliner, *Spin Labeling: The Next Millennium*, Plenum, New York, **1998**, and references therein.
[6] a) W. L. Hubbell, A. Gross, R. Langen, M. A. Lietzow, *Curr. Opin. Struct. Biol.* **1998**, *8*, 649; b) Z. F. Guo, D. Cascio, K. Hideg, W. L. Hubbell, *Protein Sci.* **2008**, *17*, 228; c) P. P. Borbat, A. J. Costa-Filho, K. A. Earle, J. K. Moscicki, J. H. Freed, *Science* **2001**, *291*, 266; d) G. Jeschke, *ChemPhysChem* **2002**, *3*, 927; e) M. Zachary, V. Chechik, *Angew. Chem.* **2007**, *119*, 3368; *Angew. Chem. Int. Ed.* **2007**, *46*, 3304; f) G. F. White, L. Ottignon, T. Georgiou, C. Kleanthous, G. R. Moore, A. J. Thomson, V. S. Oganesyan, *J. Magn. Reson.* **2007**, *185*, 191; g) C. Beier, H. J. Steinhoff, *Biophys. J.* **2006**, *91*, 2647; h) G. R. Luckhurst, *Thin Solid Films* **2006**, *509*, 36.
[7] a) A. Arcioni, C. Bacchiocchi, I. Vecchi, G. Venditti, C. Zannoni, *Chem. Phys. Lett.* **2004**, *396*, 433; b) P. J. Le Masurier, G. R. Luckhurst, *J. Chem. Soc. Faraday Trans.* **1998**, *94*, 1593.
[8] V. S. Oganesyan, *J. Magn. Reson.* **2007**, *188*, 196.
[9] H. J. Steinhoff, W. L. Hubbell, *Biophys. J.* **1996**, *71*, 2201.
[10] J. Peláez, M. Wilson, *Phys. Chem. Chem. Phys.* **2007**, *9*, 2968.
[11] a) R. Berardi, L. Muccioli, C. Zannoni, *ChemPhysChem* **2004**, *5*, 104; b) A. J. McDonald, S. Hanna, *J. Chem. Phys.* **2006**, *124*, 164906.
[12] D. van der Spoel, E. Lindahl, B. Hess, G. Groenhof, A. E. Mark, H. J. C. Berendsen, *J. Comput. Chem.* **2005**, *26*, 1701.
[13] Gausian 03, Revision E.01, M. J. Frisch, G. W. Trucks, H. B. Schlegel, G. E. Scuseria, M. A. Robb, J. R. Cheeseman, J. A. Montgomery, Jr., T. Vreven, K. N. Kudin, J. C. Burant, J. M. Millam, S. S. Iyengar, J. Tomasi, V. Barone, B. Mennucci, M. Cossi, G. Scalmani, N. Rega, G. A. Petersson, H. Nakatsuji, M. Hada, M. Ehara, K. Toyota, R. Fukuda, J. Hasegawa, M. Ishida, T. Nakajima, Y. Honda, O. Kitao, H. Nakai, M. Klene, X. Li, J. E. Knox, H. P. Hratchian, J. B. Cross, V. Bakken, C. Adamo, J. Jaramillo, R. Gomperts, R. E. Stratmann, O. Yazyev, A. J. Austin, R. Cammi, C. Pomelli, J. W. Ochterski, P. Y. Ayala, K. Morokuma, G. A. Voth, P. Salvador, J. J. Dannenberg, V. G. Zakrzewski, S. Dapprich, A. D. Daniels, M. C. Strain, O. Farkas, D. K. Malick, A. D. Rabuck, K. Raghavachari, J. B. Foresman, J. V. Ortiz, Q. Cui, A. G. Baboul, S. Clifford, J. Cioslowski, B. B. Stefanov, G. Liu, A. Liashenko, P. Piskorz, I. Komaromi, R. L. Martin, D. J. Fox, T. Keith, M. A. Al-Laham, C. Y. Peng, A. Nanayakkara, M. Challacombe, P. M. W. Gill, B. Johnson, W. Chen, M. W. Wong, C. Gonzalez, J. A. Pople, Gaussian, Inc., Wallingford CT, **2004**.
[14] H. J. C. Berendsen, J. P. M. Postma, A. DiNola, J. R. Haak, *J. Chem. Phys.* **1984**, *81*, 3684.
[15] B. Hess, H. Bekker, H. J. C. Berendsen, J. G. E. M. Fraaije, *J. Comput. Chem.* **1997**, *18*, 1463.
[16] T. Darden, D. York, L. Pedersen, *J. Chem. Phys.* **1993**, *98*, 10089.
[17] U. Essmann, L. Perera, M. L. Berkowitz, T. Darden, H. Lee, L. G. Pedersen, *J. Chem. Phys.* **1995**, *103*, 8577.

Received: May 24, 2010
Published online: September 8, 2010

